SAND2010-1618C

Expansion of a Tungsten Carbide – Epoxy Composite Following Hypervelocity Impact

C.S. Alexander[*] [a], T.J. Vogler [b], T.F. Thornhill [c], W.D. Reinhart [a]
[a] *Sandia National Laboratories, Albuquerque, NM 87185, USA*
[b] *Sandia National Laboratories, Livermore, CA 94550, USA*
[c] *K-Tech Corporation, Albuquerque, NM xxxxx, USA*

Received Date Line (to be inserted by Production) (8 pt)

Abstract

The behavior of a shocked tungsten carbide - epoxy mixture as it expands into a vacuum has been studied through a combination of experiments and simulations. X-ray radiography of the expanding material as well as the velocity measured for a stood-off witness plate are used to understand the physics of the problem. The initial shock causes vaporization of the epoxy matrix, leading to a multi-phase flow situation as the epoxy expands rapidly at around 8 km/s followed by the WC particles moving around 3 km/s. There are also small amounts of WC moving at higher velocities, apparently due to jetting in the sample. In addition to the experiments, two-dimensional mesoscale simulations of the shock and expansion processes were conducted. These simulations give results that are in reasonable agreement with experimental results. More importantly, they provide insight into the physics of the problem and can be used to explore sensitivities. In particular, they suggest that energy release by epoxy plays an important role in the expansion process.

Keywords: Article, Template, Instructions, HVIS. (please enter 4 or 5 keywords, 10 pt)

1. Introduction

The phenomenon of multi-phase flow is important to a variety of applications. In order to gain a greater understanding of the physical processes occurring under these conditions, a composite of tungsten carbide (WC) particles suspended in an epoxy matrix was studied through a combination of hypervelocity impact experiments and numerical simulations.

Experiments conducted using the two-stage light gas gun facility at Sandia National Laboratories consist of a Lexan slug traveling at approximately 6 km/s impacting a tungsten carbide-epoxy (WCE) composite target. The impact is sufficient to vaporize the epoxy in the target while the WC particles remain in the solid phase providing the multi-phase conditions. The expansion of the WCE target following impact is observed with flash x-rays as well as witness plates monitored with VISAR

*Corresponding author. Tel.: +1 505 845 3572; fax: +1 505 844 8467.
E-mail address: calexa@sandia.gov

interferometry. Results of these experiments show that the epoxy expands rapidly at around 8 km/s followed by the WC particles traveling at around 3 km/s. In addition, small amounts of WC are observed to move at greater velocities apparently due to jetting in the sample.

In order to better understand the experimental results, a series of two dimensional mesoscale simulations of the shock and expansion process were conducted. Results of these simulations are in good agreement with the experimental results and provide insight into the important physical processes of the problem. In particular, the results indicate non-uniformity in the initial shock and in the expansion of the epoxy ahead of the WC particles. Further, non-uniformities observed in the WC particle distribution are similar to the apparent jets seen experimentally. The results also suggest that energy release by the epoxy plays an important role in the expansion process.

Additional one dimensional simulations were performed in order to probe the response of the expanding epoxy. Results indicate that the expansion front traveling at around 8 km/s has a density on the order of 0.001 g/cc. The density of the epoxy gradually increases behind this front to approximately 0.01 g/cc while the velocity decreases to 4-5 km/s.

2. Experimental Techniques

2.1 Material

The WCE studied was fabricated using the same WC powder from Kennametal, Inc., studied by Vogler *et al.* [1]. Individual particles consist of single WC crystals produced through a melt process [2]. The particles were sieved to give nominal particle sizes in the range of 20-32 μm. Epon 828 resin and Epi-Cure Z curing agent were used at a ratio of 5:1 by mass. A nominal volume fraction of WC particles of 45.3% was used. Based on a density of 1.20 g/cm^3 for the epoxy and 15.7 g/cm^3 for WC, one expects a density of approximately 7.77 g/cm^3. The mixture was vacuum outgassed before and after pouring into molds. The molds were heated to 93° C over 10 hours, then held at that temperature for 10 hours before cooling to room temperature over an hour. After curing, approximately 1 mm was machined from the top and bottom of each WCE billet to remove resin-rich and resin-poor regions, and then samples were machined from the billets. The material produced consists primarily of isolated WC particles surrounded by epoxy with few, if any, voids present. Samples were machined to be flat and parallel to approximately 13 μm. Contact surface profilometry indicates an average roughness value, Ra, of approximately 1 μm with isolated low points on the order of 10 μm deep that are suggestive of WC particles that have pulled out of the surface.

After fabrication, each sample disk was characterized for nominal density based on volume and mass, and the longitudinal and shear wave speeds of the material were measured at the center and four points between the center and edge distributed around the disk. The average density was 7.77 g/cm3, while the average longitudinal and shear wave speeds were 2.04 and 1.12 km/s, respectively.

2.2 Experimental Setup

Experiments were conducted in three formats: Hugoniot state measurement, expansion with x-rays, and expansion with witness plate. Specifics for the experiments are given in Table 1. Each configuration provides different information about the behavior of the material. However, since the

impact velocities for all experiments were within 1% of the average, the experiments can be considered identical except for variability in density between samples.

Table 1. Summary of experimental configurations

Shot	*Velocity (km/s)*	ρ_o *(g/cm3)*	*Sample Thick. (mm)*	*Instrumentation*	*X-ray Times*[1] */ Witness Plate Configuration*
WCE-6	5.953	8.162	3.06	VISAR / LiF window	N/A
WCE-17	5.924	7.707	4.08	X-rays	4.007 μs, N/A
WCE-14	5.976	8.177	4.08	X-rays	7.829 μs, 90.717 μs
WCE-8	5.976	7.626	4.06	X-rays	10.326 μs, N/A
WCE-18	5.830	7.760	4.07	X-rays	N/A, 64.017
WCE-15	5.960	7.607	4.07	203 mm x 1.5 mm witness plate / VISAR	47.8 mm from back of sample
WCE-16	6.008	7.716	4.06	254 mm x1.5 mm witness plate / VISAR	91.52 mm from back of sample

1 Times given with respect to impact

In the first configuration, illustrated in figure 1a, standard shock physics techniques were used to measure the Hugoniot state in the WCE sample. Two small holes were drilled through the WCE sample opposite the centerline from one another and toward the edge of the impacted zone, and a small LiF window (6 mm diameter) was placed in each hole such that it was flush with the front face of the WCE sample. The WCE sample was backed by a larger 19 mm diameter window. A thin layer (approximately 3000 angstroms) of aluminum was vapor plated onto the front of the LiF windows. Coaxial shorting pins on the back surface of the sample (not shown in figure) provided instrumentation trigger upon impact as well as a measurement of projectile tilt. Typically, tilt was less than 8 mrad. The velocity of the plated surfaces was then monitored using VISAR diagnostics. The measurements at the front of the sample provide the time of impact, while the VISAR on the back of the sample give the time for the shock to travel through the sample. This information can be used to determine the Hugoniot state as described in Section 3.1.

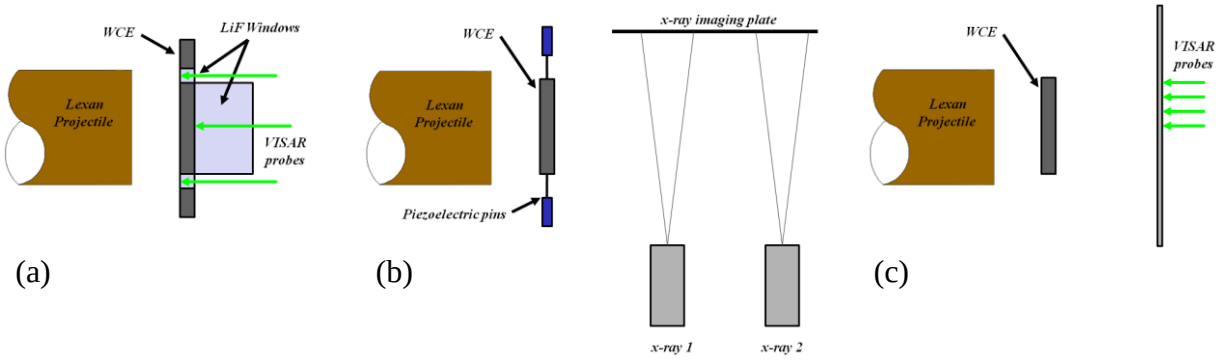

Fig. 1. Schematic diagram of the three experimental configurations; (a) shock Hugoniot, (b) expansion with x-ray diagnostics, and (c) expansion with a witness plate.

In the second configuration, illustrated in figure 1b, a 25 mm diameter sample is held between three piezoelectric pins at the end of an aluminum cylinder mounted on the two-stage gas gun as shown in Fig. 3. The three pins provide a trigger for the instrumentation with minimal contamination of the experiment. The sample was impacted with a Lexan cylinder then allowed to expand into the vacuum of the gun's tank. Two 150 kV flash x-rays oriented perpendicular to the axis of the gun were placed about 200 mm apart. Times for the x-ray flashes relative to impact are given in Table 1; each x-ray pulse was approximately 24 ns long.

The third configuration, illustrated in figure 1c, is similar to the second except that a 1.5 mm thick witness plate was used instead of x-rays to probe the expansion process. The witness plates were placed at 48 and 92 mm from the back of the sample. The back of the witness plate was monitored with five independent VISAR beams along the centerline and radially away from the center at 8.6, 17.3, 25.9, and 34.5 mm.

3. Experimental Results

3.1 Determination of the shock Hugoniot state

Experiment WCE-6 was performed to determine the shock state for the experiments reported herein. Two VISARs at the edge of the sample monitoring the impact plane and a third monitoring the back of the sample were used to determine the shock velocity. Records from these three probes are shown in Fig. 2. The difference of about 24 ns in the shock times for the two edge records is due to tilt of about 7 mrad in the impactor. The difference between the average time for the edge records and the center record of about 471 ns gives a shock velocity U_s of 4.32 km/s. By impedance matching with the Lexan impactor, the Hugoniot state is found to be u_p = 1.34 km/s, σ = 47.2 GPa, and ρ = 11.83 g/cm^3. This analysis assumes that the shock wave is steady as it traverses the sample, which may not be correct if significant amounts of energy are being released during that process and the wave is growing in amplitude in a process similar to a detonation process.

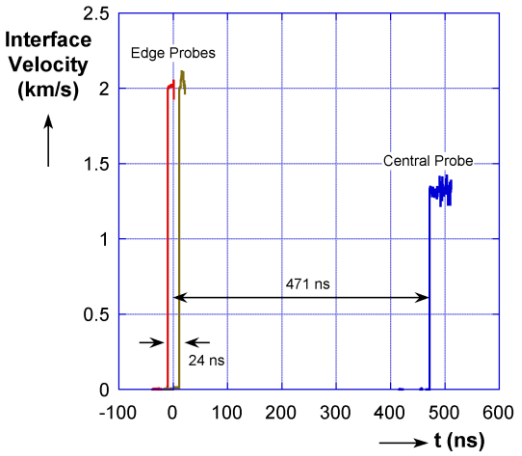

Fig. 2. WCE-6 velocity histories measured with VISAR.

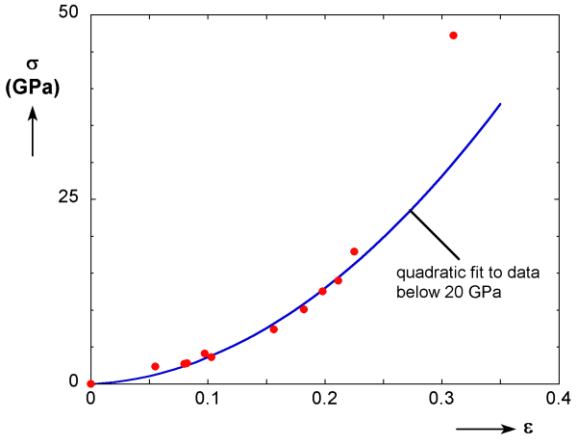

Fig. 3. WCE Hugoniot from shock experiments. The line represents a quadratic fit to data below 20 GPa.

When the results of WCE-6 are compared to other shock experiments on WCE, the result appears significantly stiffer than for the lower pressure regime as shown in Fig. 3. Here, the solid line is a quadratic fit to the low-pressure data; the data point for WCE-6 falls significantly above this line, though it is a large extrapolation from 20 GPa to 46 GPa. Previous studies of epoxy have shown that it disassociates at a shock pressure of around 25 GPa [3]. Thus, the epoxy is expected to be completely disassociated in this experiment. The epoxy may also be releasing significant amounts of energy as suggested by the stiffer response in Fig. 3

3.2 Expansion Experiments with X-Ray Diagnostics

X-ray radiography was conducted on four experiments varying the timing and positioning of two independent x-ray flashes. Each test was conducted under nearly identical impact conditions to allow for compilation of the results. As indicated in table 1, these four tests resulted in five useful x-ray images taken from 4 - 90 μs after impact.

Images taken from 4.007 - 10.326 μs after impact are shown in figure 4. Note that the scaling is different in each image in order to show more detail. A comparative image compilation at a uniform scale is shown later in figure 7. The WC particles in the WCE sample form a very dark region that is relatively uniform in the center and curls around at the outer edges. Recall that the X-ray is a 2-D projection of an axisymmetric event. In addition, a small amount of WC particles are observed to move ahead of the main group. These will be discussed further later. The lighter region surrounding the WC particles is the lower density Lexan projectile. The projectile is observed to expand radially and flow around the target. This is not surprising given initial diameters of 30.2 mm for the projectile and 25.4 mm for the WCE target. Thus, the Lexan initially flows unimpeded past the sample, but as the WC expands laterally it pushes the Lexan outward. The three piezoelectric pins used to hold the target are also visible in the images indicating the approximate location of the target prior to impact.

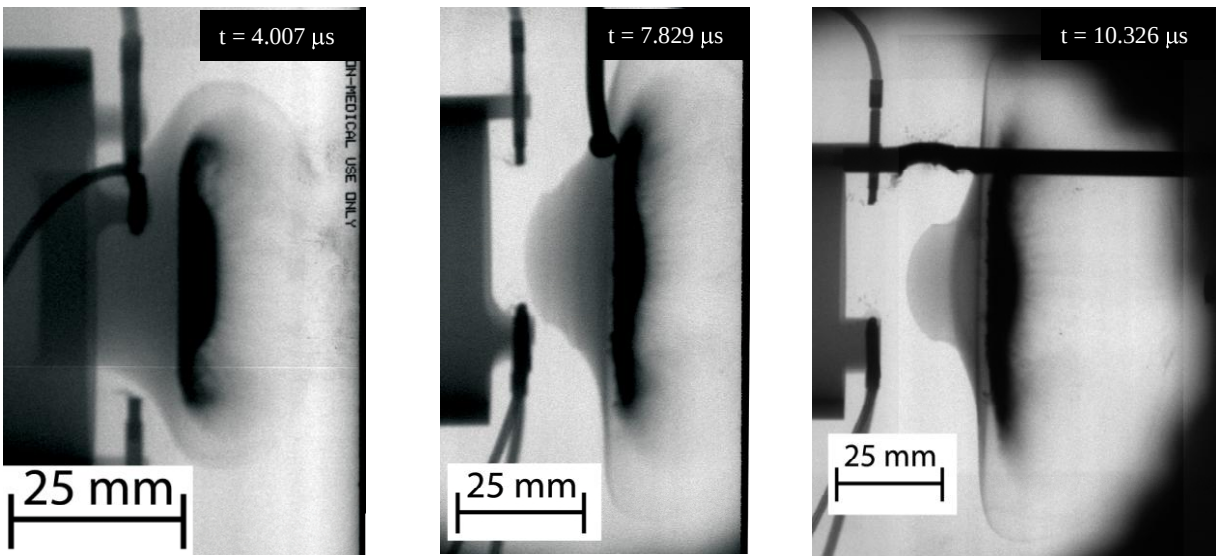

Fig. 4. X-ray images taken at shown times following impact.

The expansion process illustrated in figure 4 continues beyond the images shown. An additional image taken 64.017 μs after impact, a time sufficient to allow much greater expansion, is shown in figure 5. Here the target fixture is no longer visible in the image as WC particles have moved approximately 230mm downrange. In this x-ray, the region of WC has expanded further both horizontally and vertically. In fact, it has spread out enough in certain regions that structures in the WC cloud can be distinguished. Distinct non-uniformities can be seen on both the front and the back, though the jets observed earlier in time seem to have spread out too much to be distinguished. To the left of the WC, the remains of the Lexan impactor can be seen.

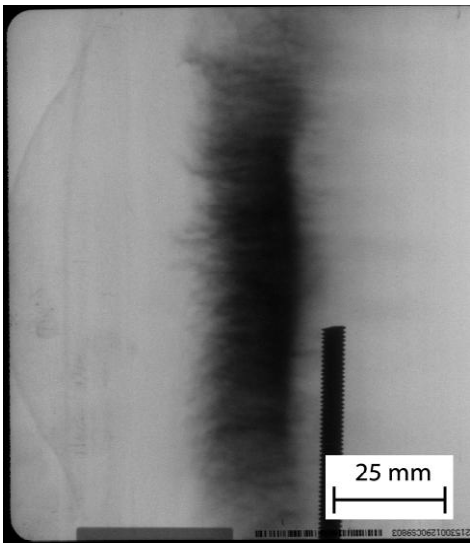

Fig. 5. X-ray image at 64.017 μs after impact.

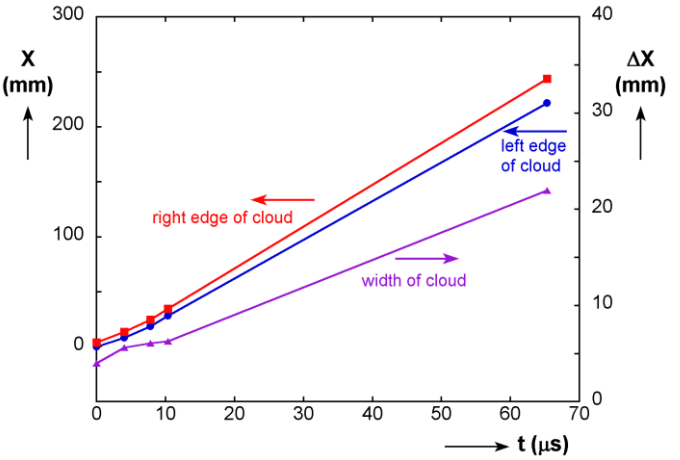

Fig. 6.Position and width of the WC cloud along the centerline for all experiments relative to time of impact.

The images in figure 4 and 5 have been analyzed to determine the location of the expanding WCE sample as a function of time. Both the leading (right) and trailing (left) edges of the main WCE region are tracked as well as the thickness. These results, shown in figure 6, illustrate that most of the changes in velocity occur in the first 8 μs after impact. The on-axis expansion of the WC at late time could be extrapolated reasonably well based on the data from 7.8 and 10.3 μs. Additional data between 20 and 60 μs would fill in the details of the expansion, but would likely not change the general picture of what is occurring.

From the data of figure 6 the velocity of the WC cloud is determined. Based on the data at 7.8 μs and beyond, where the cloud appears to have reached a steady of expansion, the leading edge velocity is 3.8 km/s while the trailing edge moves at 3.5 km/s. Thus the cloud spreads at a rate of 300 μm/μs.

The presence of a few WC particles ahead of the main WC group can be seen in the data. The origin of these faster-moving particles is not clear. They may be due to ejection of particles from near the surface of the original sample, or they might be caused by non-uniformities in the material leading to jetting of material out the back of the sample. While it is difficult to distinguish the details of the jets, they appear to be spaced at an interval of 2-3 mm. Initially, the jests move at a much greater speed than the WC cloud (3.2 km/s versus 2.5 km/s for the leading edge of the cloud at 4 μs) the difference

becomes smaller at later times. The jets have slowed to about 3.9 km/s at 64 μs after impact and appear to be approaching an equilibrium velocity with the leading cloud edge.

To better illustrate the evolution of the WC region, the images from the three experiments are shown together in figure 7. The images are well placed in time to show the expansion process without overlapping one another. The radial expansion of the WC at a nearly constant rate is evident, as is the horizontal expansion in the central region. The central region of the WC initially flows in a 1-D manner, but edge release allows increasing amounts of radial expansion, so that by about 8-10 μs the entire sample has transitioned from 1-D flow and the rate of radial expansion is approximately constant. The width of the WC region also increases, but the increase is not necessarily uniform due to the transition from 1-D flow. The region at the edge of the sample is curled over due to the flow of the Lexan impactor around and past the target. Finally the material ahead of the main group of WC appears to be increasing in density, but this may be a shot-to-shot variation in the x-ray exposure.

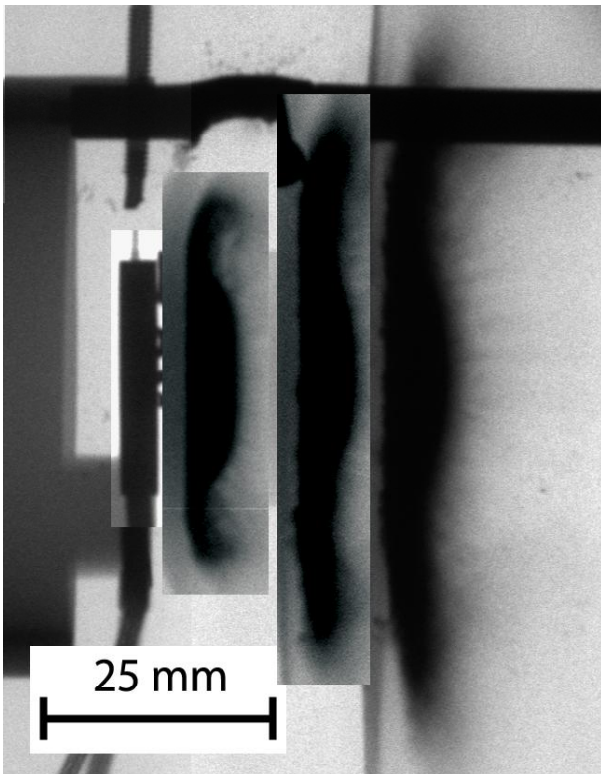

Fig. 7. X-ray radiographs of the WC expanding at 4.007, 7.829, and 10.326 μs after impact. Also shown is a WCE sample prior to impact.

3.3 Expansion Experiments with Witness Plates

In two experiments, WCE-15 and WCE-16, 1.5 mm thick aluminum witness plates were placed 47.8 and 91.5 mm, respectively, from the back of the WCE sample. The motion of the rear surface (right side in figure 1c) of the witness plate was then monitored using VISAR along the centerline and

at multiple points extending radially from the center. Representative data from WCE-15 is shown in figure 8. In both experiments, initial motion is recorded corresponding to material moving at about 8 km/s, probably vaporized epoxy that expands from the back of the target. Such material was not visible in the X-rays, but witness plates are better suited to capturing this low-density material. At later times, the VISAR records become increasingly jagged, perhaps due to impact WC particles forming the jetting region. Eventually, the light returned by the VISAR drops to a negligible level suggesting impact of the main WC cloud.

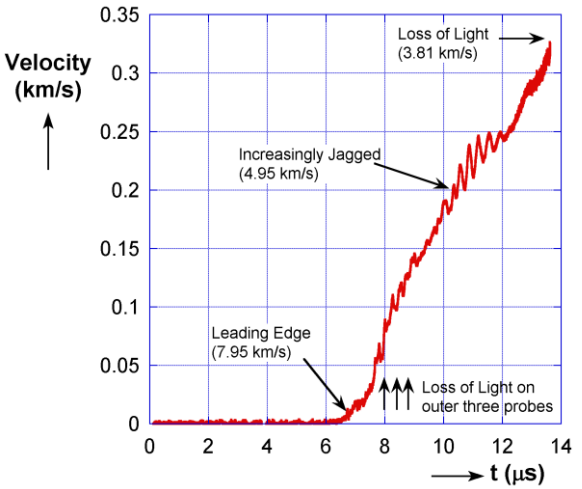

Fig. 8. Velocity history record along the centerline of the witness plate for WCE-15 located 47.8 mm downrange of the target.

In contrast to the centerline measurement, the probes positioned radially lose light much earlier as indicated by arrows in figure 8. The probe at 17.3 mm shows an initial response similar to the centerline probe but then loses light at about 7.5 μs, while the 25.9 and 34.5 mm probes lose light at about 8.0 and 8.5 μs, respectively. This suggests the witness plate in that region is being struck by something more substantial than vaporized epoxy. It is likely that the Lexan projectile outside of the sample diameter is impacting the witness plate and causing light to be lost prematurely. Loss of light at 7.5 μs would indicate a velocity of 7.0 km/s (accounting for the thickness of the target). Although this is somewhat higher than the projectile velocity of 6 km/s, it still appears to be the most likely explanation for the loss of light. Energy input from vaporizing the epoxy could explain the increase in velocity of material in front of the expanding WCE.

4. Mesoscale Modeling Results

4.1 Modeling WCE Expansion

In order to gain additional insight into the behavior observed in the experiments, two-dimensional mesoscale simulations of the experiments were conducted using CTH. Similar simulations have been

performed for WC powder [4], sand [5], and WCE [6]. The simulations performed here consist of 32 μm diameter circles of WC randomly distributed in the domain to give the proper volume fraction. Surrounding the WC particles was an epoxy matrix. A simple Mie-Grüniesen EOS is used for the WC, and it is assumed to behave in an elastic-perfectly plastic manner with a yield strength of 8 GPa. A tabular EOS, Sesame 7602, was used for the epoxy, and the Lexan impactor was assumed to have the same EOS.

The impactor was assumed to be in contact with the target at time t=0 was assigned an initial velocity of 6 km/s. Dimensions for the simulations were a sample 3 mm wide and 1 mm tall, with the impactor 6 mm wide and 1 mm tall. Periodicity conditions were applied to the top and bottom of the simulation domain so that the simulation behaves as if it is infinitely tall.

Part of the simulation domain is shown in figure 9. Images (a-c) shown on the left, illustrate the shock loading of the WCE sample after impact. The top part of each image shows contours of pressure while the bottom part shows contours of velocity. Image (a) shows the domain at the beginning of the simulation; the solid colored region to the left is part of the impactor. The second image, (b), shows the simulation after 0.22 μs. A shock wave is seen about 1 mm into the sample. Some non-uniformity is observed in the wave front, and the wave itself is seen to have a finite thickness. By 0.7 μs (c), the wave has traversed the sample and has started to emerge from the back surface of the sample.

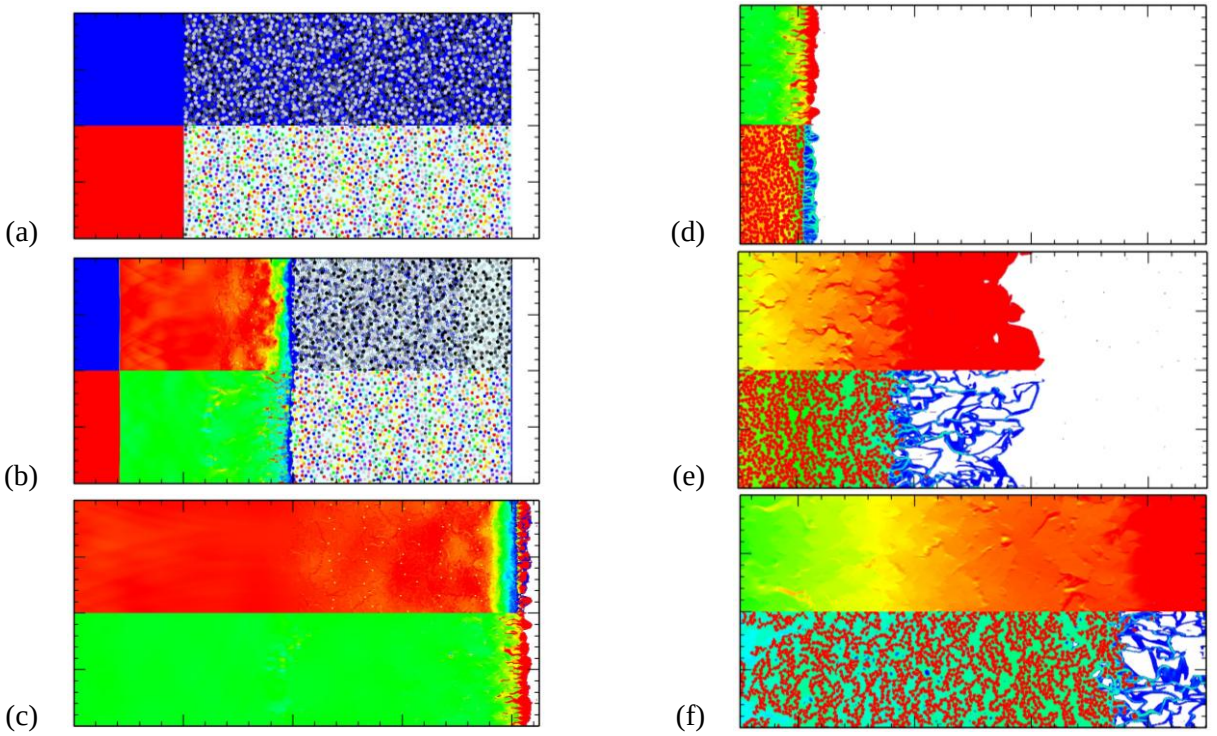

Fig. 9. Mesoscale simulation results shown at t=0.00 (a), 0.22 (b), 0.70 (c,d), 1.00 (e), and 1.70 (f) μs. The top part of each image shows contours of velocity while the bottom part shows density contours. The lowest density shown is 0.01 g/cm^3.

The expansion process is illustrated in figure 9 (d-f) shown on the right. In these images the top part of each image shows contours of velocity while the bottom part shows density contours. Image (d)

is at the same time as (c) but the perspective is shifted to the right. At 1.0 μs (e), the WC particles have moved nearly a millimeter, but the epoxy material has moved nearly two millimeters. Materials with a density of less than 0.01 g/cm^3 are omitted from the lower part of the model, resulting in tendrils of material. These tendrils would look somewhat different for different choices of this lowest contour value. By 1.7 ms (f), the edges of the expanding epoxy have moved beyond the field of view, and almost all of the WC is visible. In fact, one particle has already exited the field of view. At the right of image (f), one can see three regions where particles are moving faster than elsewhere. These regions, as well as the single particle off the field of view, seem consistent with the apparent jetting seen in figures 4 and 7. At this point, the width of the main body of WC particles is approximately 3.4 mm, so it has already expanded somewhat and will expand further at later times. The leading edge of the epoxy, based upon the 0.01 g/cm^3 contour, travels at approximately 6.3 km/s, though choosing a lower value for the contour is expected to result in a higher velocity.

Densities were extracted from the mesoscale simulations at specific times and averaged vertically through the domain. These average density profiles are shown in Fig. 10. At the beginning of the simulation, there are some fluctuations in the density due to small variability in the positioning of the particles. At 2 μs after impact, the WC region is still compressed somewhat due to the initial shock, but it is now expanding. At 4 μs, the WC region has expanded to about 4.4 mm, which is somewhat lower than the width measured in WCE-17 of 5.7 mm. However, this measurement was made at a density of about 3.2 g/cm^3. Examination at lower densities gives a greater width; it is not clear what density the boundary in the x-ray data corresponds. It is also worth noting that any misalignment between the WC region and the axis of the x-ray tube will make the WC appear wider than it really is, though that effect appears to be relatively small in WCE-17. The leading edge of the dense region has moved about 9.1 mm in the simulation, while in WCE-17 the leading edge has moved about 9.8 mm. Thus, the results of the mesoscale simulations agree quite well with the experimental results at 4 μs. At later times, radial expansion effects become more significant and the lack of that expansion in the simulations makes the comparison between the experiments and simulations less valid.

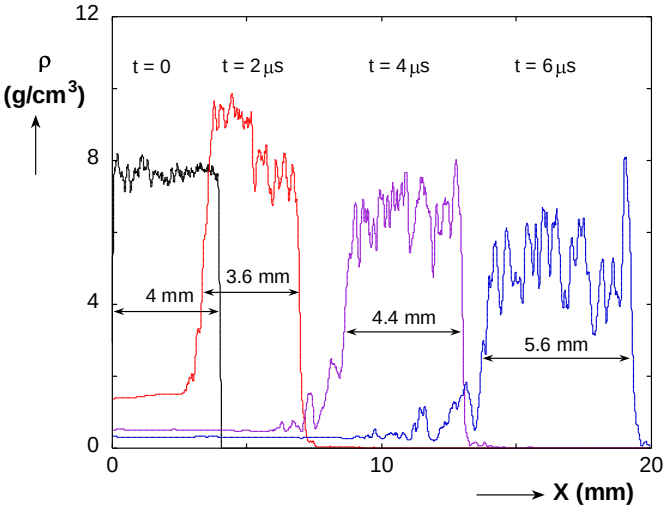

Fig. 10. Density averaged vertically across the Mesoscale simulation at t=0, 2, 4, and 6 μs after impact.

4.2 Reactive vs. Non-Reactive Epoxy Models

The Hugoniot results in Section 3.1 suggest that the epoxy matrix may release significant energy in these experiments. Also, once a polymer such as epoxy is heated sufficiently, it is important to account for the condensation products properly [7]. Unfortunately, there is no reactive model available in CTH for epoxy. To assess the effects of reactivity, simulations were performed with PMMA (Sesame 7750) substituted for epoxy. The two polymers have similar initial densities, and a reactive model is available for PMMA that utilizes the HVRB model to link the EOSs of PMMA and the reaction products [3]. The EOS for the PMMA reaction products is denoted as Sesame 7752.

Mesoscale simulations were conducted using a non-reactive EOS for PMMA as well as a reaction model. Simulations with non-reactive PMMA are quite similar to those shown in figures 9 and 10. However, reactive models behave differently, at least in the leading edge of the expanding material for densities below about 1 g/cm^3 as can be seen in figure 11. The leading edge for the reactive model is moving noticeably faster than that of the no-reactive model for low densities. Densities are plotted on a logarithmic scale in figure 12 to highlight the differences between the non-reactive and reactive models for densities typical of gases, ~0.001 g/cm^3. The front of the reactive model at that density is moving significantly faster than the non-reactive model, with the difference increasing for lower densities. Comparing the profiles for 2 and 3 μs at a density of 0.001 g/cm^3, the velocity for the non-reactive and reactive models are 6.3 and 6.7 km/s, respectively. Thus, the reactive model gives results closer to those seen experimentally, though the velocities from the simulations are somewhat slower. This may be due to differences between PMMA and epoxy in the reaction regime.

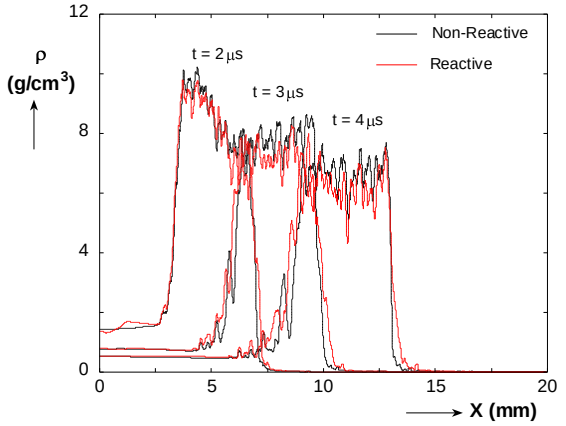

Fig. 11. Density averaged vertically across the mesoscale simulations using non-reactive and reactive models for PMMA at t = 2, 3, and 4 μs relative to impact.

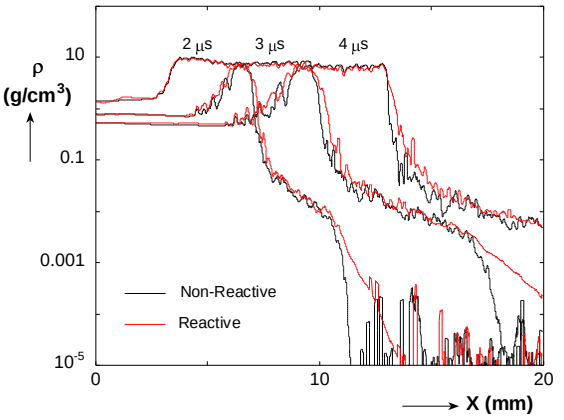

Fig. 12. Density data of figure 11 plotted on a logarithmic scale to show detail at low density.

4.3 Estimate of Leading Edge Gas Density

Low-density gases are not visible in the x-rays, but the witness plate experiments record an integrated measure of density and velocity. In order to estimate the density of the gas hitting the witness plate, one-dimensional simulations were conducted in which a 1.5 mm thick layer of aluminum

was impacted with a thick layer of low-density material traveling at 8 km/s. The first EOS utilized for the low-density material was air with an initial density of 0.001 and 0.0001 g/cm^3. Velocity histories from the simulations (shifted 6 μs) are compared to those from experiment WCE-15 in Fig. 23. The simulation results show a stair step pattern as waves reverberate in the aluminum plate, accelerating it at a nearly constant rate. The fall-off after about 10 μs is an artifact relating to the finite size of the simulation. The acceleration caused by 10^{-4} g/cm^3 air is relatively low, while that due to 10^{-3} g/cm^3 air is similar to that seen experimentally. Thus, it seems likely that the leading edge of the expansion detected with the VISAR is on the order of 0.001 g/cm^3. Densities lower than that are unlikely to accelerate the witness plate enough to be detected. In order to examine higher densities than air at ambient pressure, PMMA at low densities was used instead. For a small value of pressure, the temperature of the PMMA was adjusted until the desired density was achieved. PMMA with an initial density of 0.001 g/cm^3 gives results quite similar to those for air at the same density. Thus, the most important parameters for the expanding material are its density and its velocity, with the composition and temperature of secondary importance.

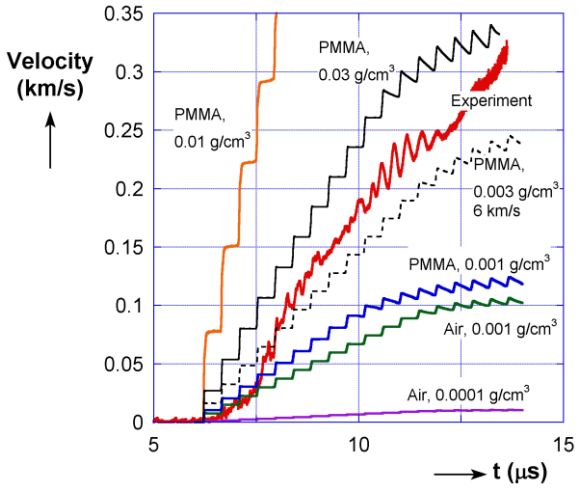

Fig. 13. Velocity histories from the back of a 1.5 mm thick aluminum witness plate for experiment WCE-15 and one-dimensional simulations at varying density and velocity conditions

Following the initial acceleration, the witness plate accelerates more rapidly after about 7.5 μs. Using 0.003 g/cm^3 PMMA gives a velocity history quite similar to that seen experimentally. If the same simulation is performed with an initial velocity of 6 km/s, then the acceleration is significantly reduced. Of course, the actual behavior in the experiment is much more complicated than these simulations. First, there is expected to be a gradient in density with the lowest density material moving fastest and the denser material moving slower. Second, the actual experiments include lateral expansion of material during the expansion process and after it impacts the witness plate. Nevertheless, these simulations provide insight into the nature of the expanding material as it strikes the witness plate. Material at about 0.001 g/cm^3 represents the leading edge detected by the VISAR. Following that, the material is increasingly dense and moving more slowly. Densities on the order of 0.003 to 0.01 g/cm^3

probably account for most of the measurements from the VISAR. In principal, one could utilize a more complex distribution of densities and velocities to recover the velocity histories seen in WCE-15 and WCE-16. However, unless radial expansion is accounted for, such an exercise is probably of limited value.

5. Conclusion

In this investigation, the behavior of a mixture of tungsten carbide and epoxy as it is shocked to nearly 50 GPa and then allowed to expand into a vacuum has been studied. This expansion process is monitored using flash x-rays and stagnation on a witness plate at a distance behind the WCE target.

The shocked WCE expands into the vacuum when the shock wave reaches the back of the sample. Gas from disassociated epoxy travels out from the sample at around 8 km/s, followed by the WC particles. The front edge of these particles moves at 2.5-3 km/s, with jetting material moving even faster, on the order of 4 km/s faster. The back edge of the particle group moves more slowly, resulting in a gradual broadening of the WC particle region. As late as 64 μs after impact, the WC particles continue to be grouped fairly closely, though that grouping has expanded both longitudinally and radially. Non-uniformities in the particle distribution also develop at such late times.

Two-dimensional mesoscale simulations of the experiments provide valuable insight into the physics of the experiments and give good quantitative agreement with the experiments. The simulations show non-uniformities in the initial shock, expansion of low density matrix material ahead of the WC particles, and the presence of non-uniformities in the WC particle distribution that are similar to the apparent jets seen experimentally. The width of the WC region and the velocity of the expanding material is somewhat lower than the experiment, however, probably due to an inadequate description of the behavior of epoxy during the shock / release process. In particular, the potential release of energy by epoxy when it is shocked to the levels seen here may play an important role in the expansion process. Finally, one-dimensional simulations suggest that the initial expanding material that reaches the witness plate at 8 km/s has a density on the order of 0.001 g/cm^3. The material gradually increases in density and decreases in velocity to somewhat less than 0.01 g/cm^3 traveling at 4-5 km/s.

Acknowledgements

The authors would like to thank Steve Montgomery for supplying the tungsten carbide-epoxy studied in this investigation. This project was supported by the Joint DoD/DOE Munitions Technology Development Program. Sandia is a multiprogram laboratory operated by Sandia Corporation, a Lockheed Martin Company for the United States Department of Energy's National Nuclear Security Administration under contract DE-AC04-94AL85000.

References

[1] T. J. Vogler, M. Y. Lee and D. E. Grady, *Int. J. Solids Structures* **44**, 636-658 (2007).
[2] E. Lassner and W.-D. Schubert, *Tungsten: Properties, Chemistry, Technology of the Element,*

Alloys, and Chemical Compounds. (Kluwer Academic / Plenum Publishers, N.Y., 1999).
[3] G. I. Kerley, Report No. KPS99-4, 1999.
[4] J. P. Borg and T. J. Vogler, *Int. J. Solids Structures* **45**, 1676-1696 (2008).
[5] J. P. Borg and T. J. Vogler, *Int. J. Impact Eng.* **35**, 1435-1440 (2008).
[6] T. J. Vogler, C. S. Alexander, J. L. Wise, S. T. Montgomery and D. E. Grady, *J. Appl. Phys.*, (in preparation) (2009).
[7] R. N. Mulford, D. C. Swift, N. E. Lanier, J. Workman, R. L. Holmes, P. Graham and A. Moore, presented at the Shock Compression of Condensed Matter - 2007, 2007 (unpublished).